2016

Self-learning Backlash Inverse Control of Cooling or Heating Coil Valves Having Backlash Hysteresis

Jie Cai
Ray W. Herrick Laboratories, Purdue University, United States of America, cai40@purdue.edu

James E. Braun
Ray W. Herrick Laboratories, Purdue University, United States of America, jbraun@purdue.edu

Self-Learning Backlash Inverse Control of Cooling or Heating Coil Valves Having Backlash Hysteresis

Jie CAI[1]*, James E. BRAUN[1]

[1]Ray W. Herrick Laboratories, Purdue University, West Lafayette, IN, USA
cai40@purdue.edu

* Corresponding Author

ABSTRACT

Valves are widely used in HVAC systems to regulate liquid flow rate, such as hot- and chilled-water valves utilized in cooling and heating coils. These valves are typically controlled with motorized actuators where significant backlash hysteresis might exist and the backlash magnitude mostly depends on the clearance of the manufactured gearbox. Due to the hysteresis effect, unsatisfactory tracking performance results when using a conventional PI controller. To understand the control effect from the backlash hysteresis, this paper develops an emulator model for a cooling coil and valve set derived from field measurements. Based on observations of the simulation results, a self-learning backlash inverse control approach is proposed to mitigate the backlash effect with moderate modifications to a conventional PI control. In the proposed approach, a self-learning procedure is carried out at the beginning of the control implementation period to estimate the backlash magnitude for a specific valve. Then a backlash inverse block is added to an existing PI controller to compensate for the hysteresis effect residing in the valve. The validity of the proposed method was verified with both simulation and experimental tests and significant improvement was observed in the control performance.

1. INTRODUCTION

Valves are commonly used in industrial and commercial applications to regulate liquid flow rate for various purposes. In building HVAC systems, valves are employed for regulation of hot- and chilled-water in cooling and heating coils to control the heat exchange rate. For valves with automatic control capability, motorized actuators are typically utilized for driving a valve to open or close based on a control command provided by a feedback controller. Backlash type hysteresis often exists in an actuator gearbox where the stem position differs at a given input command when the actuation changes its direction, causing difficulties in obtaining a stable control. The hysteresis magnitude depends on the manufacturing clearance that can vary significantly even for the same batch of products.

This study was motivated by the unsatisfactory comfort control that had been observed in the HVAC system serving multiple offices that are Living Laboratories for the Center for High Performance Buildings at Purdue University. The unsatisfactory performance was mainly caused by valve hysteresis residing in the chilled- and hot-water valves. Conventional PID controllers were not able to provide stable control due to the valve hysteresis and the control variables were observed to oscillate significantly. As a consequence, space temperatures fluctuated and comfort requirements could not be satisfied. A companion paper (Cai, Kurtulus and Braun, 2016) presented a comprehensive set of experimental test results comparing different valve characteristics in variable-air-volume (VAV) box reheat and air handling unit (AHU) cooling coil valves and investigated their impacts on control performance. The results showed severe control temperature fluctuations for valves having significant backlash-type hysteresis. In addition, the control fluctuations led to unnecessarily high cooling/heating power so demand costs would be raised for buildings subject to demand charges. Backlash-type hysteresis commonly exists in HVAC valves due to the relatively low manufacturing tolerances employed and emphasis on low cost solutions. All position controlled valves that were surveyed in Cai et al. (2016) suffered from significant backlash hysteresis (more than 5%). Thus, a specifically devised control approach for handling such backlash-type hysteresis could bring tremendous benefits for buildings in energy cost reduction and improved comfort.

Backlash inverse control has been studied extensively in the control community as an effective approach to mitigate backlash-type hysteresis in a control system. The backlash inverse controller is typically implemented in series with a typical feedback controller, e.g., PI controller, to compensate for backlash-type non-linearity. For systems with unknown backlash sizes, adaptive inverse control is often utilized to estimate and adapt the backlash size (Tao and Kokotovic, 1993, Tao and Kokotovic, 1996 and Ahmad and Khorrami, 1999). However, most of the adaptive laws in the previous work are only valid for linear systems and very few studies considered case studies with nonlinear plants.

Hagglund (2007) proposed an on-line estimation algorithm for backlash magnitude based on closed-loop operation data. The on-line estimation step achieved a similar goal to the self-learning process proposed in the current study. But the estimation mechanism is different: Hagglund (2007) utilized the delay time and magnitude in the system reaction to infer the backlash size that requires information of the PI control settings and estimation of the plant static process gain. In addition, the backlash estimation quality highly depends on external disturbances. The self-learning process within the present paper, however, is based on simple observations in the control behavior and no information is needed in terms of plant characteristics or PI control settings. In addition, it is more robust in handling external disturbances.

Some previous research work studied dynamic modeling of hydronic valves with hysteresis to enable controller design and performance assessment. For example, Kumar and Mittal (2010) developed a dynamic model of the liquid flow process within a regulation valve. A hysteresis model was incorporated to capture the hysteresis effect and the overall model provided a simulation test bed to investigate different valve control approaches. Tudoroiu and Zaheeruddin (2005) considered a similar case study as the present paper where the valve backlash hysteresis effect on control performance of a discharge air temperature system was studied. The paper relied on a dynamic simulation model to investigate the backlash effect and fluctuations were observed in the discharge air temperature when valve backlash magnitude was increased gradually. However, the study mainly focused on the fault detection problem without addressing the control problem.

This paper focuses on the development of data-driven cooling coil and valve models that are useful in understanding control stability issues caused by valve hysteresis and in developing controllers to mitigate the backlash hysteresis effect leading to improved control performance. Based on the observed control chattering patterns, a self-learning approach is proposed to estimate the backlash magnitude and a corresponding backlash inverse controller is implemented to improve the control performance. The effectiveness of this approach has been demonstrated via both simulation and experimental tests although only simulation results will be presented in this paper due to space limitations. Note that the proposed self-learning backlash inverse control approach is generally applicable for hydronic valves although only a HVAC application is demonstrated here.

2. VALVE AND COOLING COIL DATA-DRIVEN MODELS

A valve model with hysteresis effects and a dynamic cooling coil model were developed based on field measurements from the Living Labs at Purdue University. Details of the experimental setup were presented in the companion paper by Cai, Kurtulus and Braun (2016). These models are combined in a simulation tool for understanding, developing and validating the backlash inverse control approach.

2.1 Valve Models

2.1.1 Valve hysteresis model: the actuation of valve opening in response to control command follows a dynamic behavior because of the inherent hysteresis where the valve opening does not only depend on the current control command but also requires information of the previous control action to determine the current actuation status in the backlash region (on the increasing or decreasing curve or in between, as shown in Figure 1 (a)). A discrete-time backlash dynamic model can be formulated as

$$
\begin{aligned}
&\textbf{If } \{cmd[t]-cmd[t-1] \geq x_{BL}-x[t-1]\} \\
&\quad x[t] = x_{BL} \\
&\quad open[t] = \alpha \times (cmd[t]-x_{BL}) \\
&\textbf{Elseif } \{cmd[t]-cmd[t-1] < x_{BL}-x[t-1]\} \textbf{ and } \{cmd[t]-cmd[t-1] \geq -x[t-1]\} \\
&\quad x[t] = x[t-1]+cmd[t]-cmd[t-1] \\
&\quad open[t] = \alpha \times (cmd[t-1]-x[t-1]) \\
&\textbf{Else} \\
&\quad x[t] = 0 \\
&\quad open[t] = \alpha \times cmd[t]
\end{aligned}
\tag{1}
$$

where t is the time step index, cmd is the model input and also the valve control command, x is a state of the dynamic system that represents the position within the backlash curves (increasing or decreasing curve or in between), $open$ is the model output which is the valve opening in percentage. The model has one independent parameter x_{BL}, which is the backlash magnitude while the parameter α is a dependent parameter representing the slope of the increasing/decreasing curve that can be determined by the value of x_{BL}.

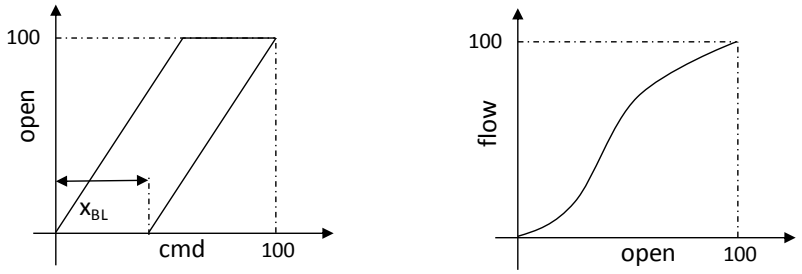

Figure 1. (a): backlash hysteresis curves. (b): valve static characteristic curve.

2.1.2 Valve static characteristic curve: there is a static characteristic curve for the valve itself that correlates the delivered flow going through the valve to the valve opening, as shown in Figure 1 (b). For equal percentage control valves, the curve typically exhibits an exponential form in the lower range and the curve becomes flat in the higher range due to loss of authority (Chapter 47 of ASHRAE Handbook-HVAC Systems and Equipment, 2012). The exact shape of the curve is dependent on the valve type, the shape of valve opening, and pressure characteristics of the hydronic system. It is difficult to find a general model form and thus, an empirical model utilizing the generalized logistic model (Richards, 1959) is used here to capture this static correlation:

$$
m = \frac{m_{max}}{\left(1+a \cdot e^{-b(open-c)}\right)^{1/a}} \tag{2}
$$

where m is the delivered flow, m_{max} is the valve nominal flow at 100% opening and $open$ is the valve opening percentage as described in the previous sub-section. Parameters a, b and c together determine the shape of the curve and their values were estimated based on training data. Parameter b determines the growth rate, c corresponds to the opening where the maximum growth rate occurs and a characterizes the asymmetrical pattern.

2.1.3 Valve model estimation: the parameters x_{BL}, a, b and c in Equations (1) and (2) were estimated simultaneously from a training data set collected from the Living Labs cooling coil valve. Within the training data, the control command (cmd) was randomly perturbed within the range of 0% to 50% (the maximum cooling command was within 45% during the year of 2015) and each perturbation was held for 5 minutes to allow the flow to reach steady state. The initial control command was started from 0% so that the experiment started on the increasing curve. Figure 2 shows the model validation results where the scatter plot on the left hand side shows the predicted and measured chilled water flow rates and the plot on the right hand side shows the data points along with the estimated curves. Very good agreement was achieved between the model predictions and actual measurements and thus, the

estimated valve model captures the valve characteristics including backlash hysteresis. The estimated backlash magnitude (x_{BL}) was close to 7%.

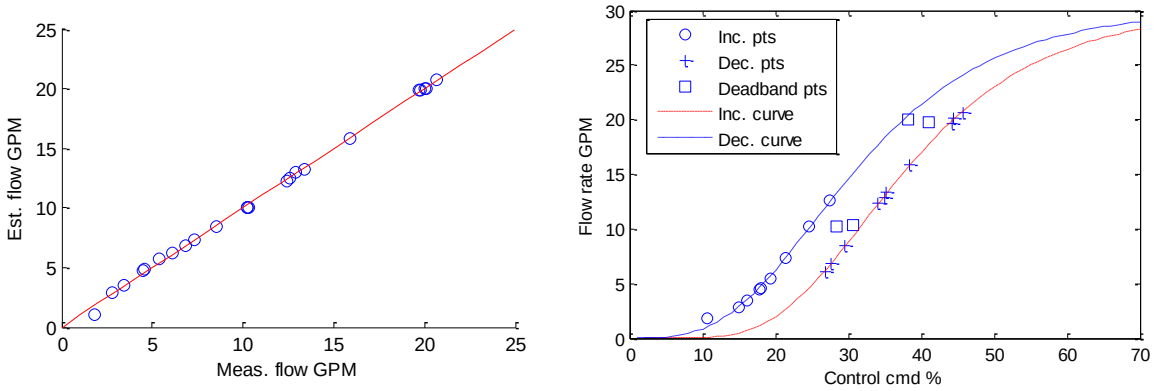

Figure 2. Left: comparison of model predictions and actual measurements. Right: data points on top of the estimated model curves.

2.2 Dynamic Cooling Coil Model

A dynamic model was established for the cooling coil where multiple key parameters were estimated from operation data collected from the Living Labs. The model was adapted from Zhou (2005) which utilizes a finite volume method with the whole cooling coil being discretized into multiple control volumes. The multi-row cross/counter-flow coil is assumed to be pure counter-flow arrangement and an effectiveness-NTU and enthalpy potential method is used to calculate heat transfer rates for each of the control volumes.

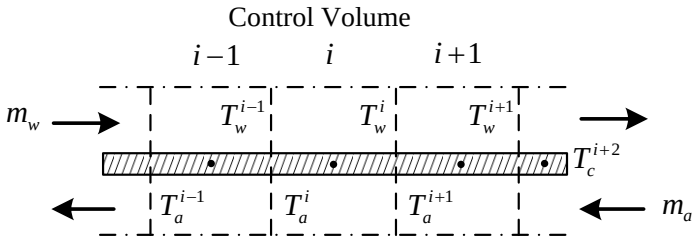

Figure 3. Control volumes in the cooling coil model

Figure 3 illustrates the finite volume method for the cooling coil under the counter-flow assumption. For each control volume, water and coil material energy balances are written in a discrete-time formulation. If no moisture is condensing on the coil surfaces within the control volume, then the resulting equations are:

$$\begin{aligned} C_w \frac{T_w^i[t+1]-T_w^i[t]}{\Delta t} + m_w c_{p,w}\left(T_w^i[t]-T_w^{i-1}[t]\right) + \frac{T_w^{i-1}[t]-T_c^i[t]}{R_w} = 0 \\ C_c \frac{T_c^i[t+1]-T_c^i[t]}{\Delta t} + \frac{T_c^i[t]-T_a^{i+1}[t]}{R_a} + \frac{T_c^i[t]-T_w^{i-1}[t]}{R_w} = 0 \end{aligned} \quad (3)$$

The variable t inside the brackets is the time step index and the superscript i indicates association to the ith control volume. Equation (3) is formulated under an explicit form to avoid solving systems of equations for each time step. However, the explicit solution scheme requires the time step to be small enough to obtain a stable solution with any given spatial discretization. The number of control volumes determines the model accuracy but is constrained by the chosen time step. The present study used 1 second as the time step and discretized the coil into 8 control volumes, which is the largest number of control volumes to reach a stable solution (for a given time step, there is a minimum spatial discretization step to achieve a stable numerical solution, which corresponds to the discretization with 8 control volumes for this specific case). This discretization granularity well leveraged model accuracy and computational requirements. Uniform temperature is assumed for the coil material in each control volume and the

air and water temperatures in each control volume are assumed to follow some steady-state profiles instead of being uniform and the effectiveness-NTU method is used for water and air side heat transfer rate calculations. T_a^i and T_w^i in these equations represent the control volume exit temperatures, which equal the inlet temperatures of the downstream control volumes. T_c^i is the bulk temperature of the coil material. C_w and C_c are thermal capacitances of the water body and coil material, respectively, inside each control volume and they are estimated parameters in the training process. m_w and m_a are water and air mass flow rates. $c_{p,w}$ and $c_{p,a}$ are specific heats for water and air, respectively. The air-side and water-side heat transfer resistances, R_a and R_w, are inverses of the effectiveness capacitance rate products that are characterized through empirical relations trained using data.

When the concerned coil section is wet (air dewpoint temperature is higher than the coil temperature), the driving potential for heat and mass transfer is enthalpy differential instead of temperature differential and thus, the following formulation is used for the coil energy balance:

$$C_c \frac{T_c^i[t+1]-T_c^i[t]}{\Delta t}+\frac{h_{s,c}^i[t]-h_a^{i+1}[t]}{R_a^*}+\frac{T_c^i[t]-T_w^{i-1}[t]}{R_w}=0\ .$$

where $h_{s,c}$ is the air saturated enthalpy at the coil temperature T_c^i and R_a^* is an air-side resistance for combined heat and mass transfer.

Dynamics in the air stream are neglected due to the low thermal inertia and the outlet air conditions for each control volume are calculated based on air side heat transfer for both dry- and wet-coil cases:

$$T_a^i[t+1]=T_a^{i+1}[t]+\epsilon_a\left(T_c^i[t]-T_a^{i+1}[t]\right).$$

where ϵ_a is an overall air-side effectiveness for heat transfer that accounts for both forced-air convection and conduction though the fin material. For dry-coil conditions, the outlet air humidity ratio stays the same as the inlet while for wet-coil conditions, the outlet air humidity is calculated with psychrometric routines based on the outlet air dry-bulb temperature and enthalpy that is calculated as follows:

$$h_a^i[t+1]=h_a^{i+1}[t]+\epsilon_a^*\left(h_{s,c}^i[t]-h_a^{i+1}[t]\right).$$

Here ϵ_a^* is an overall air-side effectiveness for both heat and mass transfer that accounts for forced-air convection, condensation, and conduction though the fin material. The air- and water-side resistances are calculated based on effectiveness correlations in terms of mass flow rates using the following forms:

$$R_a=\frac{1}{\epsilon_a m_a c_{p,a}},\qquad R_w=\frac{1}{\epsilon_w m_w c_{p,w}},\qquad R_a^*=\frac{1}{\epsilon_a^* m_a}$$

where

$$\epsilon_a=1-\exp\left(-\beta_3 m_a^{\beta_4}\right),\quad \epsilon_w=1-\exp\left(-\beta_1 m_w^{\beta_2}\right),\quad \epsilon_a^*=1-\exp\left(-\beta_5 m_a^{\beta_6}\right) \tag{4}$$

The key parameters in the model were estimated from field measurements and the estimation parameters are C_c, C_w in Equation (3) and β_1 to β_6 in Equation (4). A training data set with several random step changes in the air and water flow rates was collected for the cooling coil serving the Living Labs and the training results are plotted in Figure 4. Since the present study mainly concerns the supply air temperature behavior, regression was carried out to minimize the root mean square error between the predicted and measured supply air temperatures. All initial temperature states were assumed to be 20 ℃ and a 30-minute warm-up period was considered so that the regression process only minimized the root mean square of the errors from the 1801 second onwards. Note that both the valve and coil estimation problems involved nonlinear regressions and the Levenberg-Marquardt method (Madsen et al., 2004) was used to find the optimal parameter values. As can be seen from Figure 4, very good agreement was achieved

between the measured and predicted supply air temperatures (denoted by 'TA lvg' in the plot). Although the leaving water temperature (denoted by 'TW lvg') behavior was not accounted for explicitly in the regression process, the predicted and measured leaving water temperatures also show good agreement and the small discrepancy is believed to be attributed to sensor biases for the water and air flow rates (energy imbalance between the water and air sides). The only significant differences in water temperature occur for zero water flow rate, which would have no impact on simulation results

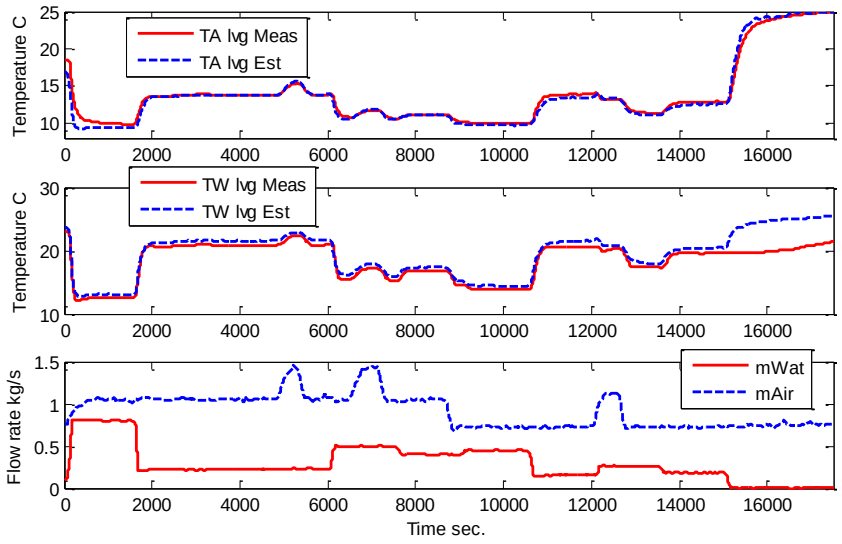

Figure 4. Model training results with artificially perturbed air and water flow rates.

To validate the model performance, a validation data set was collected under normal operation with a resetting supply air temperature strategy to reduce VAV box reheat. Figure 5 shows the validation results and good accuracy was achieved in the supply air temperature prediction even though the operating conditions differed significantly from those in the training data set.

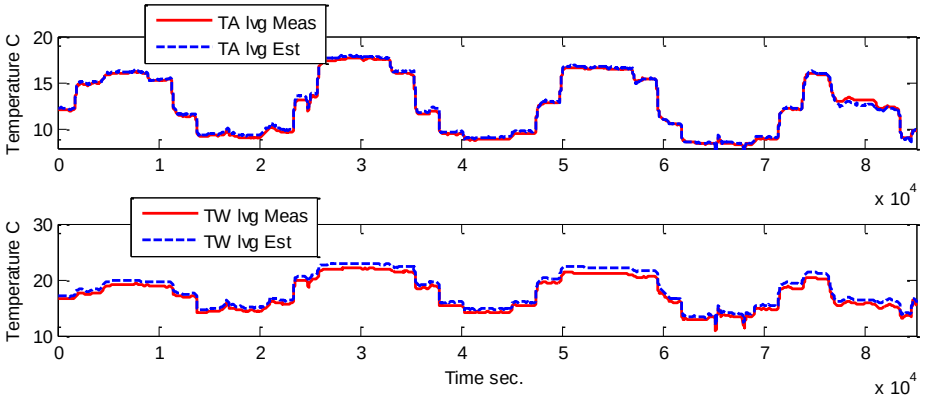

Figure 5. Cooling coil validation results with real operation data.

3. SIMULATION TESTS

3.1 Simulation Test Setup

An emulator model was constructed by combining the valve and cooling coil models developed in the preceding section. Figure 6 shows the component layout of the emulator models along with the feedback control loop. For typical cooling coil operation, a feedback controller, e.g., a PI controller, is used to generate control commands for the valve actuator to adjust valve opening so that the supply air temperature follows the setpoint. The emulator

consists of three component models developed in the preceding section: an actuator backlash model that takes the PI control command and outputs the actual valve opening; a valve static curve model translating the valve opening to water flow rate; and a dynamic cooling coil model that provides outlet air and water conditions based on the chilled water flow rate and other boundary conditions. The cooling coil outlet air temperature is used as the control variable. In the simulation tests, boundary conditions, such as airflow rate and inlet water and air temperatures, were extracted from actual measurements in the Living Labs.

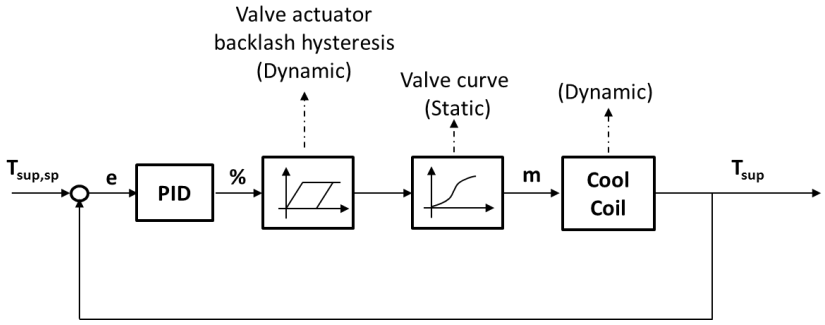

Figure 6. Simulation and control diagram.

3.2 PI Control Results

Figure 7 shows simulation results with a conventional PI controller with proportional and integral gains fine tuned by field engineers. The supply air temperature setpoint was artificially perturbed to test the setpoint tracking performance. Note that in actual system operations, resetting supply air temperature setpoint strategies are usually employed as an energy efficient option to reduce reheat in terminal VAV boxes. With the conventional PI controller, the control variable, i.e., the supply air temperature, fluctuated significantly due to the valve hysteresis.

3.3 Backlash Inverse Control Results

Figure 8 shows the backlash inverse control diagram. It simply adds a backlash inverse (BI) control block between the conventional PI controller and the control plant. The backlash inverse block is a dynamic system that is an inverse of the backlash model formulated in Equation (1) so that the net effect is unity. The backlash magnitude in the backlash inverse block should match that of the actual control plant to fully compensate for the backlash effect. However, the actual backlash magnitude is unknown so a self-learning process is proposed to adapt the backlash inverse block for a specific valve, which will be described at the end of this section.

Figure 9 and Figure 10 show the test results of backlash inverse controllers with 60% and 95% backlash magnitude estimates relative to the true valve (7%), respectively. The backlash inverse control with a 60% backlash estimate has led to reduced fluctuation in the supply air temperature compared to the baseline PI controller. However, the control action was still delayed due to the underestimated backlash size and control fluctuation still existed. The 95% backlash inverse control provided almost perfect temperature tracking as the backlash hysteresis effect was well compensated for.

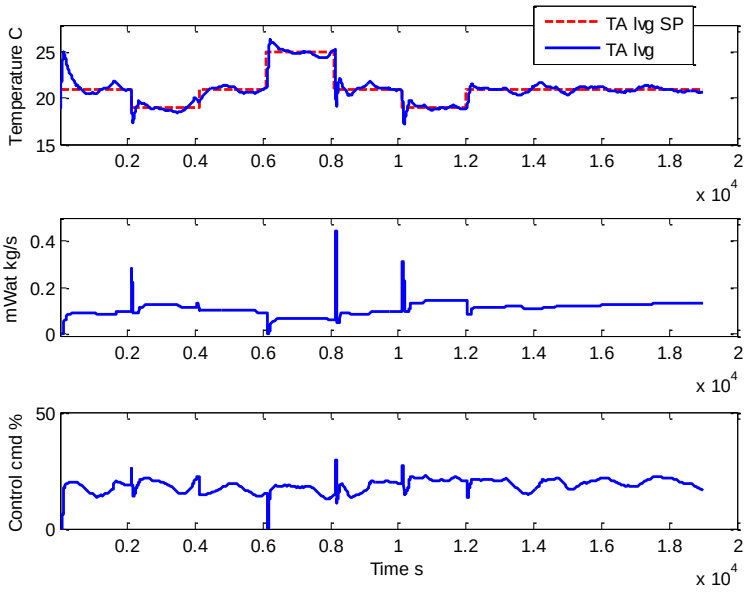

Figure 7. Conventional PI control results.

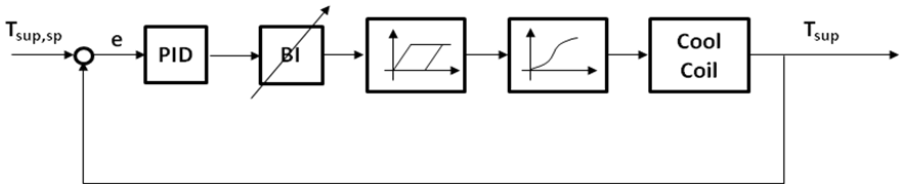

Figure 8. Backlash inverse control diagram.

Although backlash inverse control is effective in mitigating backlash hysteresis effects, an overestimated backlash could compromise the control performance with significant chattering in the control action. With an overestimated backlash, the backlash inverse controller over-compensates for the backlash effect at each switch time leading to excessive control action in the reverse direction. This leads to high frequency mode switches and control chattering. Figure 11 shows the variations of mode switch frequency and tracking error (RMSE between the setpoint and control variable) with respect to different relative backlash estimates (normalized with the actual backlash magnitude). The mode switch frequency was calculated by averaging the numbers of mode switches within each 10-minute time block. It can be seen that as the backlash estimate approaches the actual value from zero, tracking performance improves consistently with decreasing tracking RMSE. However, when the backlash estimate rises beyond the actual value, the tracking error increases as a consequence of control chattering. The mode switch frequencies shown on the left hand side of Figure 11 are relatively constant when the backlash estimate is below the actual value. Once the estimate passes the actual backlash magnitude, the mode switch frequency increases dramatically. This pattern forms the basis of the proposed self-learning process: increase the backlash estimate until significant control chattering occurs. Figure 12 shows the self-learning process for estimating the backlash size with a 0.7% (equal to 10% of the actual backlash magnitude) step adjustment. When the mode switch frequency stays within 200% of the frequency corresponding to the minimum backlash estimate (0.7% for the considered case), the backlash estimate is stepped up and if mode switch frequency goes beyond 200% of the frequency with the minimum backlash estimate, the backlash estimate is stepped down. In the demonstrated case shown in Figure 12, backlash estimate updating was performed every 30 minutes and the learning process took less than 3 hours to identify the correct backlash size. Note that the initial guess and step adjustment of the backlash estimate could take any arbitrarily small but nonzero value although the number of iterations to reach convergence will vary.

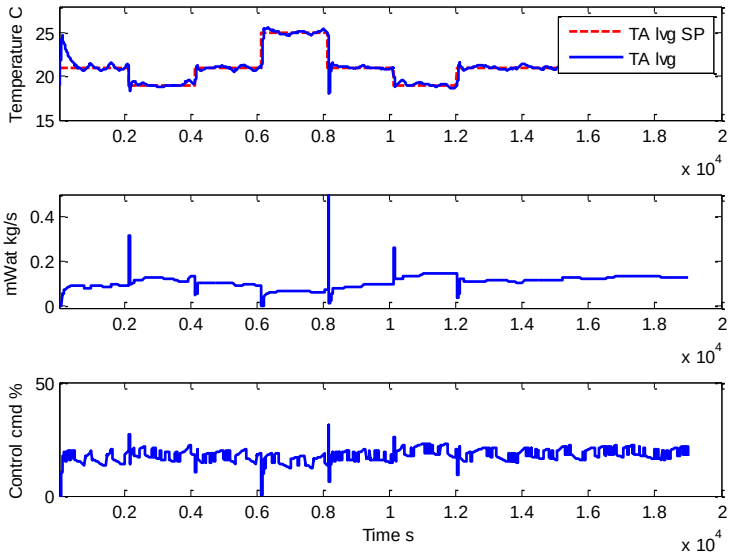

Figure 9. Backlash inverse control with 60% of the estimate.

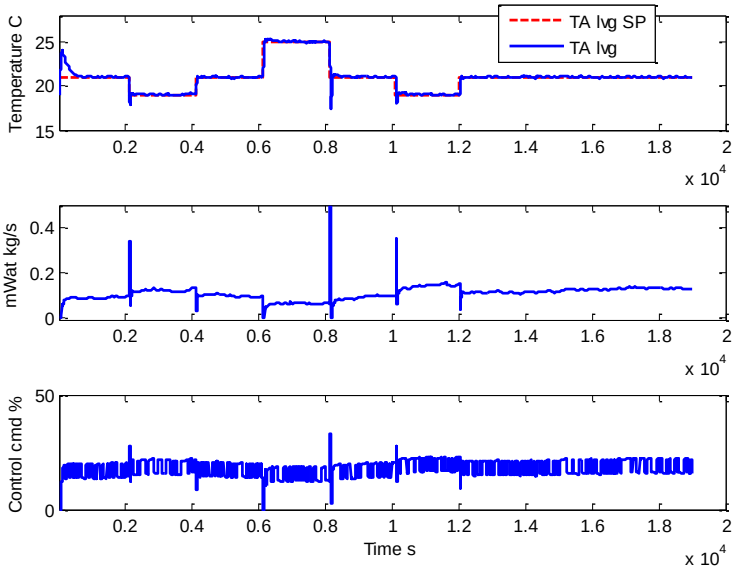

Figure 10. Backlash inverse control with 95% of the estimate.

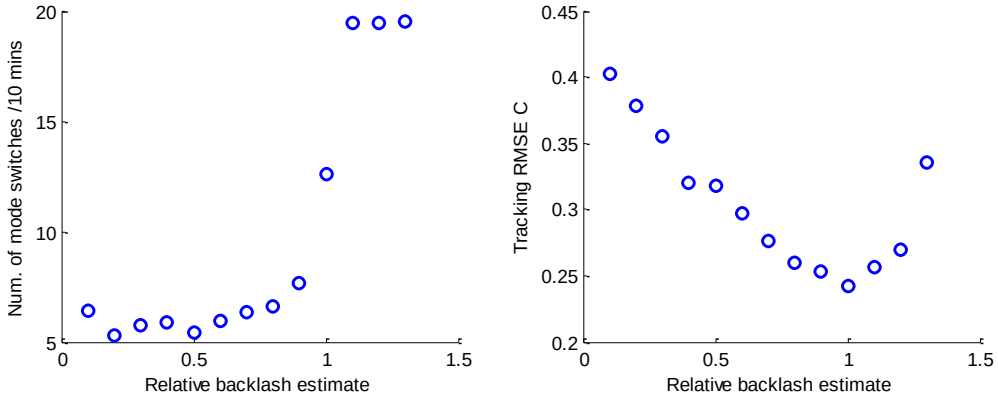

Figure 11. Control behaviors with different backlash estimates normalized with the actual backlash magnitude (7%).

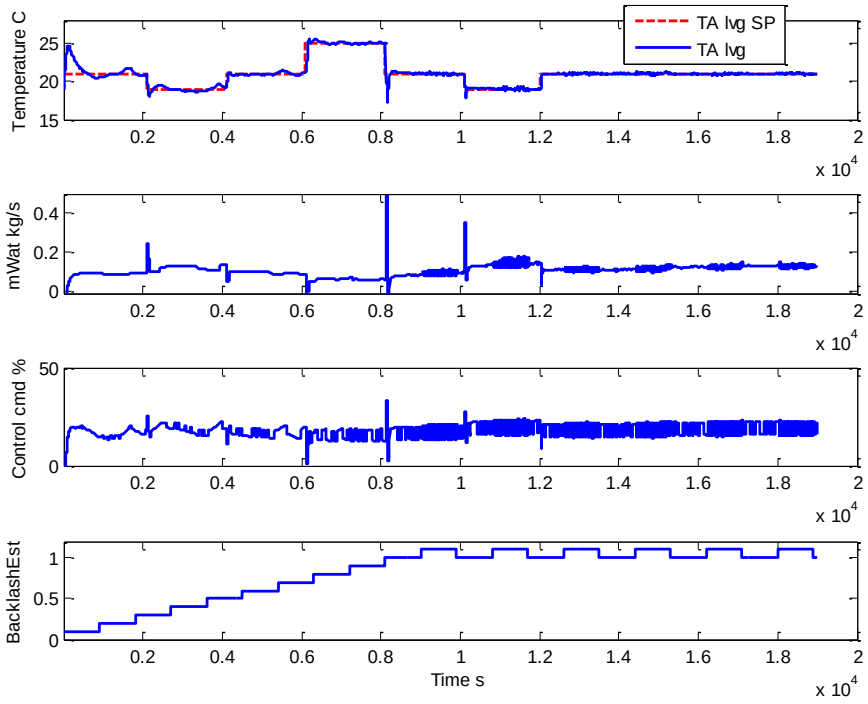

Figure 12. Self-learning process to estimate the backlash size.

6. CONCLUSIONS

This paper proposed a self-learning backlash inverse control approach to mitigate the backlash hysteresis effects associated with typical hydronic valves and to improve control performance. A specific HVAC application was considered as a case study that applied the proposed backlash inverse control approach to a cooling coil valve. To assess the control performance improvement, an emulator was constructed combining dynamic models of an actuator (backlash effect) and a cooling coil calibrated with field measurements obtained from Living Labs at Purdue. Simulation test results showed that for valves with noticeable backlash hysteresis, a conventional PI controller led to low frequency fluctuations in the supply air temperature (control variable). The proposed backlash inverse control added to a conventional PI controller demonstrated significantly improved control performance in mitigating the backlash effects and the best performance was achieved when the backlash size estimate was equal to or slightly less than the actual valve backlash. Intensive control chattering occurs when the backlash size is overestimated so a self-learning process was proposed that increments the backlash estimate from zero until significant chattering occurs. This self-learning process was tested within the emulator model and the actual backlash size was identified within three hours of operation.

The proposed backlash inverse control approach was also tested in the actual cooling coil operation serving the Living Labs. The experimental testing results showed a close match with the simulation results under both baseline and backlash inverse controls. However, the measurement noise in the experimental test induced severe mode switches. This issue was previously reported by Dean et al. (1995) where a backlash inverse controller was applied and tested within a servomotor. To overcome this issue, a buffered backlash inverse controller was proposed and the testing results showed significantly improved control performance with moderate mode switches. Due to space limitations, the buffered backlash inverse controller and the experimental testing results will be reported in future publications.

NOMENCLATURE

cmd	control command	(%)
x_{BL}	backlash magnitude	(-)
α	backlash curve slope	(-)

x	backlash state	(-)
m	mass/volumetric flow rate	(kg/s or l/s)
open	valve opening	(%)
t	time index	(-)
T	temperature	(K)
c_p	specific heat at constant pressure	(kJ/kg-K)
h	enthalpy	(kJ/kg)
R	thermal resistance	(K/W)
C	thermal capacitance	(kJ/K)
ϵ	effectiveness	(-)
Tsup/Tlvg	AHU supply air temperature	(K)

Subscript

a	air
w	water
c	coil material
sp	setpoint
max	maximum

Superscript

i	the i-th control volume
*	heat and mass transfer

REFERENCES

Ahmad, N. J., and Khorrami, F., "Adaptive control of systems with backlash hysteresis at the input." *American Control Conference*, 1999.

ASHRAE. ASHRAE Handbook- HVAC Systems and Equipment, 2012.

Cai, J., Kurtulus O. and Braun, J.E., "Experimental performance investigation of cooling or heating coil valves and their impact on temperature controls", *16th International Refrigeration and Air Conditioning Conference at Purdue*, 2016.

Dean, S.R., Surgenor, B.W. and Iordanou, H.N., "Experimental evaluation of a backlash inverter as applied to a servomotor with gear train." *IEEE Conference on Control Applications*, 1995.

Hägglund, Tore. "Automatic on-line estimation of backlash in control loops." *Journal of Process Control*, 2007.

Kumar, V. and Mittal, A.P., "Dynamic modeling of liquid-flow process due to hysteresis of pneumatic control valve", *International Journal of Intelligent Control and Systems*, 2010

Madsen, K., Nielsen, H.B. and Tingleff, O., Methods for Nonlinear Least Squares Problems, Informatics and Mathematical Modeling, Technical University of Denmark, 2004.

Tao G. and P. Kokotovic. "Adaptive control of systems with backlash". Automatica, 1993

Tao G. and P. Kokotovic, Adaptive Control of Systems with Actuator and Sensor Nonlinearities, John Wiley & sons, 1996

Tudoroiu, N., and M. Zaheeruddin, "Fault detection and diagnosis of valve actuators in HVAC systems." *IEEE Conference on Control Applications*, 2005.

Zhou, X., Dynamic modeling of chilled water cooling coils, Ph.D. dissertation, Purdue University, 2005.